Neutron scattering investigations on the effect of crystallization temperature and thermal treatment on the chain trajectory in bulk-crystallized isotactic polystyrene

Jean-Michel Guenet
Centre de Recherche sur les Macromolécules (CNRS), 6 rue Boussingault, 67083 Strasbourg Cédex, France
(Received 1 July 1980; revised 24 September 1980)

Small-angle neutron scattering (SANS) investigations coupled with differential scanning calorimetry (d.s.c.) have been performed on isotactic polystyrene (IPS) samples crystallized in bulk by one of three thermal treatments: crystallization at high supercooling ($T_c = 140°C$); crystallization at low supercooling ($T_c = 200°C$); crystallization at $T_c = 140°C$ then annealing at $T_{an} = 180°C$. The neutron scattering experiments show that the chain trajectory in the semcrystalline medium varies depending on the molecular weight of the protonated matrix and the crystallization process. The SANS data, interpreted in the light of the d.s.c. measurements and conformational models of the semicrystallized chain, point out in particular that the size of the regularly-folded crystalline sequences (along the 330 plane) increases with chain mobility in the originally amorphous melt. These results are quite consistent with those of previous studies of IPS using bulk-crystallized samples and solution-grown single crystals.

INTRODUCTION

The study of chain trajectory in semicrystalline polymers is a topical problem. The recent use of small-angle neutron scattering (SANS) has allowed the determination of chain conformation by isotopic substitution. During the past few years, a large body of neutron scattering data has been gathered[1-4] on semicrystalline polymers. Experiments performed on polyethylene, after minimizing the isotopic segregation occurring in the course of crystallization, have shown that the radius of gyration of the chain in the semicrystallized bulk has a value close to that measured in the molten state[1]. This experimental result has been widely commented upon, in particular by Yoon and Flory[5]. Using numerical computations based on a Monte Carlo simulation, they propose conformational models wherein regular folding does not take place. However, these models suffer from non-physical characteristics such as anomalous density in the disordered region or negative dimensions for the amorphous links as shown by Guttman *et al.*[6] with numerical computations and by Guenet[7] with analytical calculations. According to these authors[6,7], the only way to account for the invariance of mean dimensions is to introduce a substantial amount of regular folding.

Experiments performed on isotactic polystyrene (IPS) seem much more promising[4,8]. In contrast to polyethylene, isotopic segregation does not occur during crystallization so that the conformational study of the isolated chain is facilitated whatever the range of scattering vectors. Depending on the molecular weight of the hydrogenated semicrystalline matrix, two sorts of result have been obtained for samples crystallized at 185°C[4].

(i) In an hydrogenated matrix of intermediate molecular weight ($M_w = 4 \times 10^5$), the radius of gyration of the labelled chain varies as $M^{0.78}$ and for the highest tagged chain molecular weight it increases by about 35%. These results have been interpreted with a conformational model designated ACA (*Figure 1a*) which is made of a large crystalline sequence incorporated along the 330 plane and two amorphous wings. This model is also supported by the scattered intensity behaviour in the intermediate range.

(ii) In an hydrogenated matrix of high molecular weight ($M_w = 1.7 \times 10^6$), the same results as those published on polyethylene have been obtained, i.e. invariance of the mean dimensions after crystallization. According to analytical calculations available in ref 7, this result has been interprated with a conformational model designated as the garland model (*Figure 1b*) made up of N_s identical subunits containing a short, regularly-folded crystalline sequence with approximately 5 rods and a disordered sequence.

The existence of different conformations in bulk-crystallized samples is supported by viscoelastic considerations according to a criterion proposed by Flory and Yoon[9]. It consists of comparing the long relaxation time, τ_m, of the chain in the originally amorphous melt to the time τ_p needed for the crystalline growth front to envelope the dimensions of one chain. If τ_m is much larger than τ_p only local rearrangements are possible leading to a garland-type model. In contrast, if τ_m is much smaller than τ_p, one may envisage a regular rearranged structure. For IPS, we obtain $\tau_m \simeq \tau_p$ for $M_w = 4 \times 10^5$ and $\tau_m \gg \tau_p$ for $M_w = 1.7 \times 10^6$. Thus, the viscoelastic behaviour is consistent with the neutron scattering results and shows that chain conformation in the semicrystalline bulk is mainly influenced by chain mobility in the melt. Such an assumption is confirmed by SANS experiments performed on solution-grown single crystals (here $\tau_m \ll \tau_p$). The results

0032-3861/81/030313-08$02.00

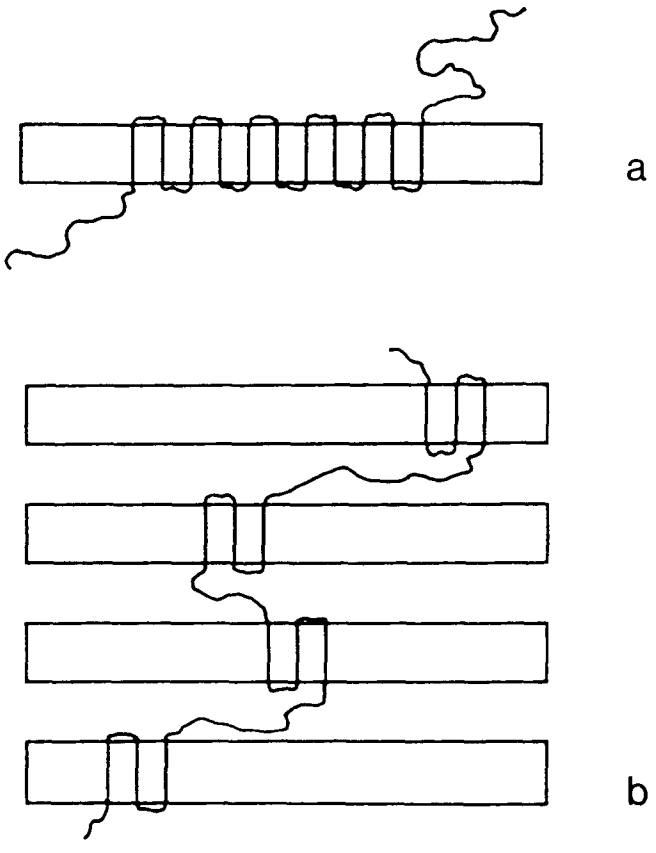

Figure 1 (a) ACA model; (b) garland model

provided by these systems are consistent with a sheet-like conformation. This means that the entire chain is regularly-folded in the lamella along the 330 plane of the crystalline lattice.

The purpose of this paper is to present new SANS experiments carried out on originally amorphous samples crystallized at high and low supercoolings using protonated matrices of different molecular weights in order to extend the previous studies[4]. The case of samples crystallized at high supercooling then annealed at higher temperature will be also presented. Moreover, d.s.c. measurements have been carried out on the semicrystallized samples for the determination of thermal behaviour.

THEORETICAL

Before presenting and discussing the experimental results, some theoretical considerations on scattering by specific semicrystalline conformations are presented. As the analytical calculation of the entire pattern of the scattered intensity is not possible, only the behaviour in the Guinier and in the intermediate ranges are examined in detail.

Radius of gyration (Guinier range)

In the Guinier range, the intensity scattered by an object of mean square radius of gyration $\overline{R_g^2}$ may be written:

$$I(q) \sim 1 - \frac{q^2 \overline{R_g^2}}{3} \qquad (1)$$

It is therefore essential to evaluate $\overline{R_g^2}$ which is directly available from experiments.

In previous papers, the expressions for radius of gyration for the ACA model[10] and garland model[7] have been analytically derived as functions of crystalline parameters and chain molecular weight.

ACA model. Calculations lead to[10]:

$$\overline{R_g^2} = (3-2y)y^2 \overline{R_p^2} + y\overline{r_e^2} + (1-y)^2(2+y)\frac{\overline{R_A^2}}{2} \qquad (2)$$

where y is the weight fraction of the crystalline sequence which includes loops joining rods. If the sample is morphologically completely crystallized and characterized by the absence of free amorphous chains, y is expressed as $y = x/z$, in which x is the crystallinity of the sample and z the weight fraction of rods in the crystalline sequence. Alternatively, $\overline{R_p^2}$ which is related to the crystalline sequence, reads:

$$\overline{R_p^2} = z^2 \frac{M^2}{M_r^2} \frac{\overline{l^2}}{12} \qquad (3)$$

where M and M_r are, respectively, the molecular weights of the chain of the elementary rod; $(\overline{l^2})^{1/2}$ is the reentry length which is the distance between two consecutive rods. $\overline{R_p^2}$ can be defined precisely by considering a chain totally incorporated along an hkO plane in a single lamella of crystallinity z. Then the conformation is equivalent to a sheet of width l_c and length L_c. Accordingly, $\overline{R_p^2}$ is expressed as:

$$\overline{R_p^2} = \frac{L_c^2}{12} \quad \text{where } L_c^2 = \frac{z^2 M^2}{M_r^2} \overline{l^2} \qquad (4)$$

As a consequence, the term $y^2\overline{R_p^2}$ is the mean square longitudinal size of the crystalline sequence in the ACA model.

Finally, in equation (2), $\overline{R_A^2}$ is the radius of gyration of the chain in the completely amorphous state and $r_e^2 \simeq l_c^2/12$.

It must be emphasized that the ACA model gives rise to an exponent ν in the law $R_g \sim M^\nu$ always larger than 0.5.

Garland model. Calculations lead to[7]:

$$\overline{R_G^2} = (1-x/z)\overline{R_A^2} + \frac{Mx}{6M_r f}[(f-1)^2\overline{l^2} + l_c^2] \qquad (5)$$

where f is the number of rods in the crystalline sequence. Other symbols are the same as for the ACA model. It must be emphasized that this relation leads always to an exponent $\nu = 0.5$.

From the theoretical results obtained on the mean dimensions in the ACA and garland models, we may derive the expression for the mean square radius of gyration $\overline{R_{cc}^2}$ for a more sophisticated model (*Figure 2*) designated as the 'central core' model (Guttman *et al.*[6]). By introducing a small change which consists of replacing the pure amorphous A wings in the ACA model by semicrystalline wings of garland type, the conformation becomes identical to that drawn in *Figure 2*. Consequently, $\overline{R_{cc}^2}$ may be calculated from equation (2) by replacing $\overline{R_A^2}$ by $\overline{R_G^2}$ given in equation (5). This simple

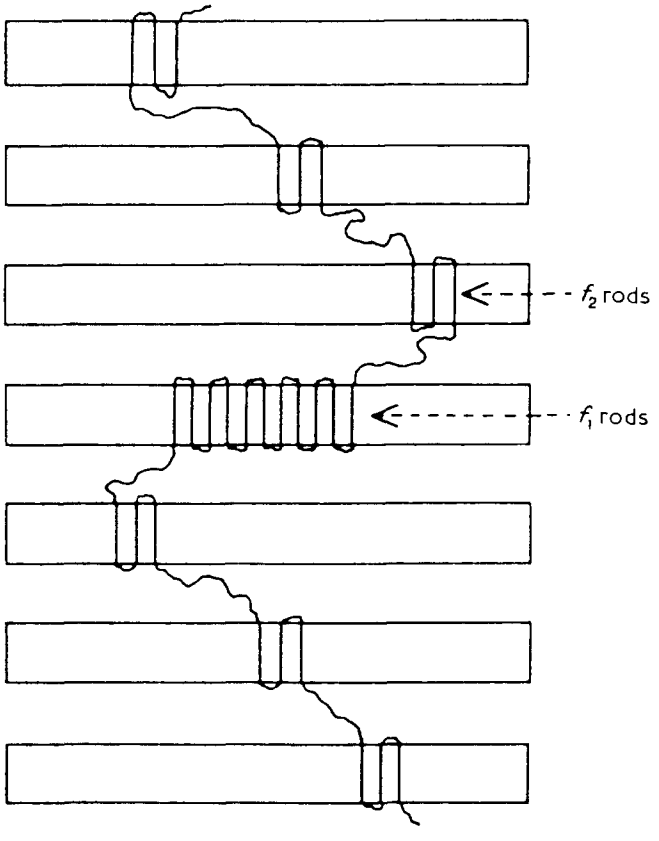

Figure 2 Central core model

procedure is possible since for both a Gaussian conformation and for the garland model the mean square dimensions are proportional to the chain molecular weight. At this stage, two kinds of 'central core' model may be considered.

(a) The number of rods situated in the central core is a constant (see ref 7). A new set of parameters is given:

y_1 = the weight fraction of the crystalline central core;
f_1 = the number of rods in the central core ($y_1 = M_r f_1 / zM$);
y_2 = the weight fraction of the crystalline sequences located in the wings;
f_2 = the number of rods in a crystalline sequence located in the garland-type wings.

The crystallinity x is then defined as:

$$x = zy_1 + (1 - y_1)y_2 \tag{6}$$

We are finally led to the expression for $\overline{R_{cc}^2}$:

$$\overline{R_{cc}^2} = (3 - 2y_1)y_1^2\overline{R_p^2} + y_1\overline{r_e^2} + (1 - y_1)^2\frac{(2 + y_1)}{2} \times \left\{(1 - y_2/z)\overline{R_A^2} + \frac{My_2}{6M_r f_2}[(f-1)^2\overline{l^2} + l_c^2]\right\} \tag{7}$$

where $y_1^2\overline{R_p^2} = (f_1 - 1)^2\overline{l^2}/12$ and is a constant.

We must emphasize that this analytical relation leads to results close[7] to those obtained by Guttman *et al.*[6] on PE by numerical computation.

(b) The number of rods in the central core depends on the labelled chain molecular weight as in the ACA model.

In such a model, only a fraction g of the crystalline sequence of the ACA model remains in the central core. The fraction $1 - g$ is distributed in the wings following the garland model. Thus, we find:

$$y_1 = xg/z \qquad \text{and } x = zy_1 + (1 - y_1)y_2$$

This leads to:

$$y_2 = \frac{x(1-g)}{1 - xg} \tag{8}$$

Hence, equation (7) may be also used for this case by replacing y_1 and y_2 by their new expressions. Here, $y_1^2\overline{R_p^2}$ reads:

$$y_1^2\overline{R_p^2} = x^2g^2\frac{M^2\overline{l^2}}{12M_r^2}$$

In contrast to the previous case, $y_1^2\overline{R_p^2}$ does depend on the chain molecular weight as found above.

Asymptotic behaviour of the form factor (intermediate range)

Usually, the intensity scattered in the intermediate range is asymptotic and of the form:

$$I(q) \sim q^{-n} \tag{9}$$

where n depends on the form factor $P(q)$ of the chain conformation. Here, the value of n is determined for the ACA and the garland models.

ACA model. The limiting value of $P_{ACA}(q)$ has been derived in a previous paper[10] and reads:

$$\lim P_{ACA}(q) = (x/z)^2 P_c(q) + \frac{1}{2}(1 - x/z)^2 P_{am}(q) + CT \tag{10}$$

in which $P_c(q)$ is the form factor of the C sequence and $P_{am}(q)$ of the A sequence. CT stand for cross-terms that are negligible for $qR \gg 1$.

Considering the A sequence as Gaussian and the C sequence as sheet-like[4,8], equation (10) becomes:

$$\lim P_{ACA}(q) = (x/z)\frac{2}{q^2 l_c L_c} + (1 - x/z)\frac{2}{q^2\overline{R_A^2}} \tag{11}$$

where l_c is the lamellar thickness, L_c is defined by equation (4) and $\overline{R_A^2}$ is the mean square radius of gyration of the chain in the totally amorphous state. From this relation, it is easy to see that the value of n is equal to 2. A further point of interest is to compare the heights of the plateaux obtained in a Kratky representation [$q^2 I(q)$ vs. q] for the ACA form factor and for a Gaussian coil form factor for a labelled chain of the same molecular weight. We find:

$$\rho_{th} = \frac{q^2 I_{ACA}(q)}{q^2 I_A(q)} = \frac{\lim P_{ACA}(q)}{P_A(q)} \tag{12}$$

Garland model. The calculation $\lim P_G(q)$ has been carried out in a previous paper[7] and reads:

$$\lim P_G(q) = (1-x/z)\lim P_A(q) + \frac{fM_r x}{Mz^2}\lim P_F(q) \quad (13)$$

where $\lim P_A(q) = 2/q^2\overline{R_A^2}$ is the asymptotic behaviour of the intensity scattered by the chain in the totally amorphous state. $\mathrm{Lim}P_F(q)$ is the asymptotic form factor of the crystalline sequence. It is clear that this relation is only valid for $qr_a \gg 1$ and $qr_F \gg 1$ where r_a and r_F are the radii of gyration of the amorphous and crystalline sequences respectively.

At this stage, taking the amorphous links to be Gaussian, two cases may be considered for the crystalline sequence.

(i) The crystalline sequence reduces to a single rod. Here $\lim P_F(q)$ reads:

$$\lim P_F(q) = \frac{\pi}{q\overline{l_c}} \quad (14)$$

in which l_c is the length of the rod and has the same value as the lamella thickness. From application of equation (13), we see that $1 < n < 2$

(ii) The crystalline sequence is made up of f rods incorporated along an $hk0$ plane.

The crystalline sequence can be regarded as sheet-like, but here l_c is the length and $(f-1)(\overline{I^2})^{1/2}$ is the width. Hence $\lim P_F(q)$ may exhibit two types of behaviour: for $ql_c \gg 1$ and $q(f-1)(\overline{I^2})^{1/2} \ll 1$:

$$\lim P_F(q) = \frac{\pi}{q\overline{l_c}}\exp -q^2(f-1)^2\overline{I^2}/24 \quad (15)$$

for $ql_c \gg 1$ and $q(f-1)\overline{I^{2\,1/2}} \gg 1$:

$$\lim P_F(q) = \frac{2\pi}{q^2 l_c(f-1)\overline{I^{2\,1/2}}} \quad (16)$$

The change in behaviour ($n < 2$ becoming $n = 2$) occurs at[8]:

$$q^* = 2/(f-1)\overline{I^{2\,1/2}} \quad (17)$$

Thus, the evaluation of q^* from experiments allows the determination of f to a first approximation provided that $\overline{I^{2\,1/2}}$ is large enough. For example, IPS, for which $\overline{I^{2\,1/2}} = 12.6$ Å, we find, respectively:

$$f = 3 \text{ and } q^* = 8\times10^{-2};\ f = 5 \text{ and } q^* = 4\times10^{-2}$$

EXPERIMENTAL

Preparation of the samples

Blends containing approximately 1% of deuterated isotactic chains of narrow polydispersity[11] were prepared from solutions in monochlorobenzene precipitated into methanol by dropwise addition. Three hydrogenated isotactic matrices have been used for these blends:

HM1 $M_w = 4.2\times10^5$ $M_w/M_n = 1.3$

HM2 $M_w = 8\times10^5$ $M_w/M_n = 2.9$

HM3 $M_w = 1.7\times10^6$ $M_w/M_n = 3$

Solid disc-shaped samples of 15 mm diameter and 1 mm thickness were first obtained in the totally amorphous state by moulding under vacuum above the melting temperature of IPS ($T_{\text{moulding}} = 250$°C) and by quenching rapidly to room temperature. Three kinds of thermal treatment have been applied to these samples:

(a) crystallization at 140°C for 5 h (matrices HM1 and HM3), samples C-140;

(b) crystallization at 200°C for 1 h (matrix HM2), samples C-200;

(c) crystallization at 140°C for 5 h then annealing at 180°C for 50 min (matrix HM1), samples C-140-A-180.

Crystallization and annealing processes have been achieved in the mould under vacuum in order to minimize the formation of microvoids.

For the determination of the mean dimensions in the pure amorphous state, isotactic protonated matrices have been replaced by atactic protonated matrices. The samples were moulded at 140° and 200°C since the IPS radius of gyration is temperature dependent in amorphous surroundings[12].

Thermal analysis

Thermal analyses were carried out using a Perkin–Elmer DSC-2 apparatus at a heating rate of 20°C min^{-1}. Approximately 5 mg of material was placed in hermetically-sealed sample pan. The crystallinity rate x of the samples has been deduced from the melting areas taking $\Delta H_{\text{IPS}} = 8.6\times10^8 \mathrm{erg\ cm}^{-3}$ [13], a value given for a perfect crystal, calibrating the experiments with indium ($\Delta H = 6.9$ cal g^{-1}).

Neutron scattering

The experiments reported in this paper were carried out at the ILL high flux reactor, Grenoble, France on D11 and D17 cameras. The scattering vectors $q = (4\pi/\lambda)\sin(\theta/2)$ ranged from:

$$5\times10^{-3} \leqslant q \leqslant 1.5\times10^{-2} \quad \text{for D11}$$

$$10^{-2} \leqslant q \leqslant 9\times10^{-2} \quad \text{for D17}$$

A mechanical monochromator was employed in both cases, providing a wavelength distribution characterized by a width at half height $\Delta\lambda/\lambda$ of about 10%.

All the results have been calibrated using a hydrogenated water spectrum. Alternatively a reference sample containing tagged chains of known molecular weight has been used[12]. Finally, the excess intensity $I(q)$ scattered by the isolated deuterated chains within the protonated matrix has been obtained by subtracting from the blend intensity $I_B(q)$ a blank signal $I_0(q)$ provided by a totally hydrogenated isotactic matrix crystallized under the same conditions.

RESULTS

D.s.c. results

Samples crystallized at 140°C (C-140). As already reported by Lemstra *et al.*[14], the thermograms (*Figures 3a* and *3b*) reveal two melting peaks ($T_{m1} = 163$°C and $T_{m2} = 197$°C) and a recrystallization peak ($T = 221$°C). According to these authors, the first peak originates from a slow crystallization process designated as secondary

crystallization. Alternatively, the thermograms are quite similar, whatever the matrix molecular weight (in this case HM1 and HM3) showing that this parameter has no influence on the morphology.

Samples crystallized at 140°C, then annealed at 180°C (C-140-A-180). The thermogram obtained on this sample (*Figure 3c*) exhibits three peaks as previously. However, the peak first located at 163°C in samples C-140 has vanished while a new peak has appeared at $T = 191$°C. In contrast, peaks located at $T = 197$°C and 221°C have not changed. The thermogram shown in *Figure 3d*, obtained on sample C-140 heated to 180°C then rapidly cooled to room temperature and heated again until complete melting, showed that the first peak disappeared leaving other peaks unchanged. This means that only the structures due to secondary crystallization have melted whereas those arising from primary crystallization have been unaffected by annealing at 180°C.

Samples crystallized at 200°C (C-200). The thermogram obtained with these samples (*Figure 4*) exhibits only two peaks, the first arising from melting and the second from recrystallization. No peak due to secondary crystallization can be detected. This agrees well with the findings of Lemstra *et al.*[14] who noted the absence of such a peak for samples crystallized at low supercoolings.

Neutron scattering results

Guinier range. Values of the mean dimensions reported in *Table 1* are significantly different depending both on the thermal treatment achieved to crystallize the samples and on the matrix molecular weight. Considering the variation of the radius of gyration with the labelled chain molecular weight, $R_g \sim M^{\nu}$, we are led to widely different exponents ν (see, for example, *Figures 5a* and *5b*).

It must be emphasized again that no isotopic segregation occurs in the course of IPS crystallization whatever the thermal treatment, contrary to polyethylene. This is shown in *Figure 6* where the neutron scattering data are plotted according to a Zimm representation for a crystallized sample (C-200 $M_{wIPSD} = 5 \times 10^5$) and the amorphous reference sample containing the same tagged chains. In such a representation, the extrapolation at $q = 0$ is directly related to the reciprocal of the weight-average molecular weight and *Figure 6* shows that this value is the

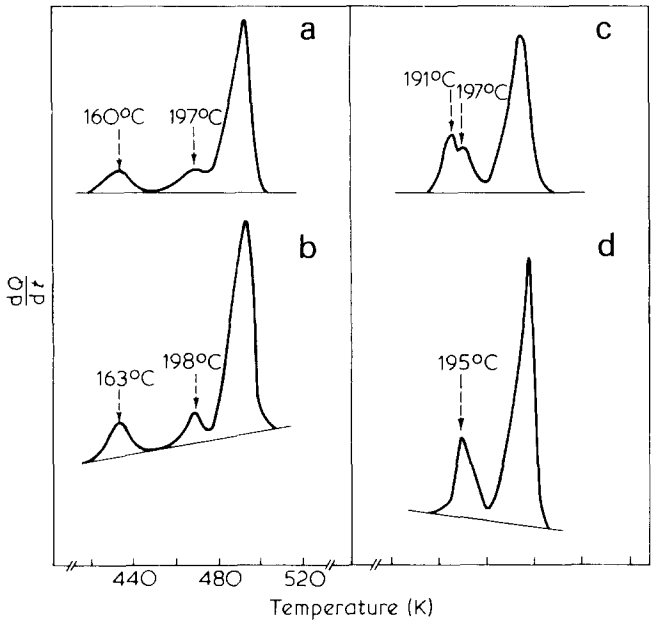

Figure 3 D.s.c. thermograms, heating rate 20°C min^{-1}. (a) Samples C–140–HM1; (b) samples C–140–HM3; (c) samples C–140–A–180–HM1; (d) sample C–140 heated until 180°C then rapidly cooled to room temperature and heated again until complete melting

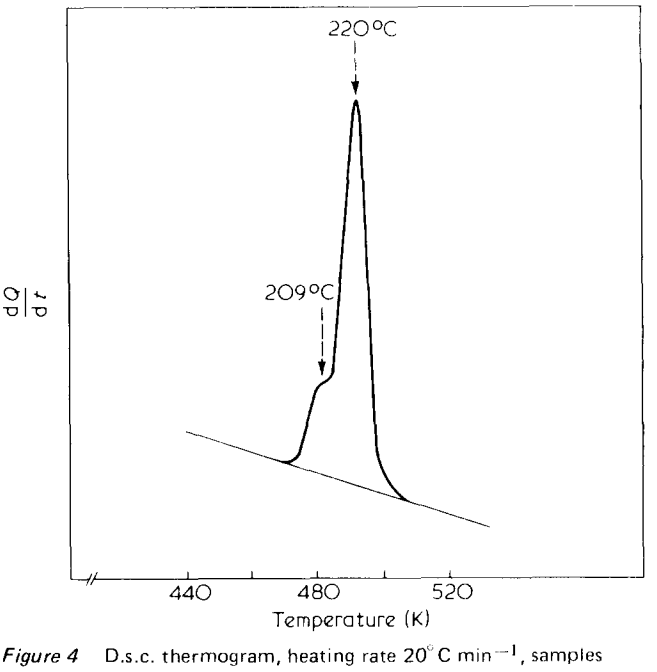

Figure 4 D.s.c. thermogram, heating rate 20°C min^{-1}, samples C–200

Table 1 HM1, $M_w = 4.2 \times 10^5$; HM2, $M_w = 8 \times 10^5$; HM3, $M_w = 1.7 \times 10^6$. Subscripts am and cry stand for amorphous and crystalline states

Sample	M_wIPSD	M_w/M_n	x	$R_{g,cry}$	ν_{cry}	$R_{g,am}$
C–140–HM1	2.5×10^5	1.15	0.34	121 ± 5	0.63	135 ± 5
	3×10^5	1.2		130 ± 6		142 ± 5
	5×10^5	1.2		172 ± 8		184 ± 8
	7×10^5	1.32		230 ± 10		217 ± 10
C–140–HM3	5×10^5	1.2	0.34	187 ± 6	0.5	184 ± 8
	7×10^5	1.32		215 ± 10		217 ± 10
C–140–A–180–HM1	2.5×10^5	1.15	0.38	133 ± 4	0.5	
	5×10^5	1.2		180 ± 5		
	7×10^5	1.32		210 ± 10		
C–200–HM2	2.5×10^5	1.15	0.34	120 ± 4	0.77	110 ± 4
	3×10^5	1.2		141 ± 5		120 ± 4
	5×10^5	1.2		206 ± 8		156 ± 6

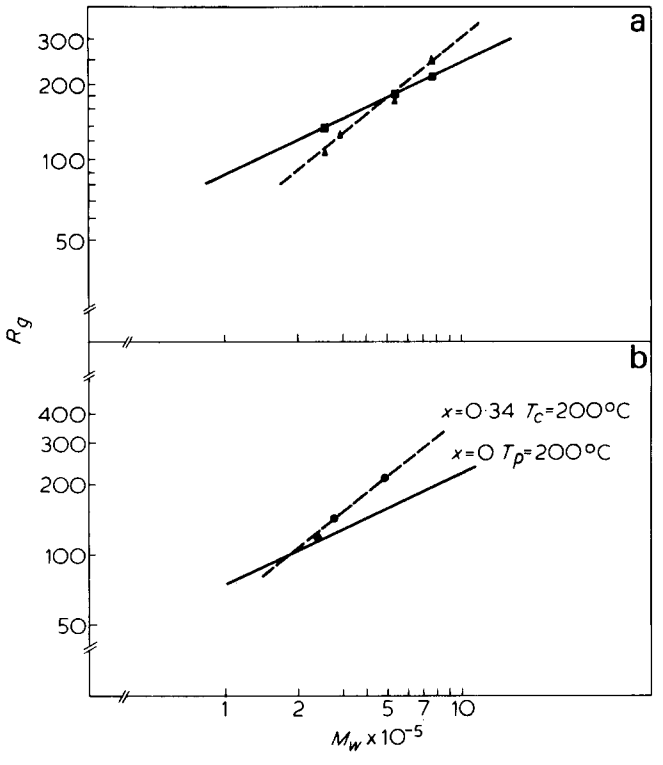

Figure 5 Log R_g vs. log M_w. (a) ▲, C–140–HM1; ■, C–140–A–180–HM1; broken line arises from results obtained on samples C–140 using a mean least squares best fit. Full line shows values obtained in the amorphous state in the atactic matrix at 140° C. (b) ●, C–200; broken line is obtained with experimental results using a mean least squares method. Full line indicates results obtained in atactic matrix at 200° C

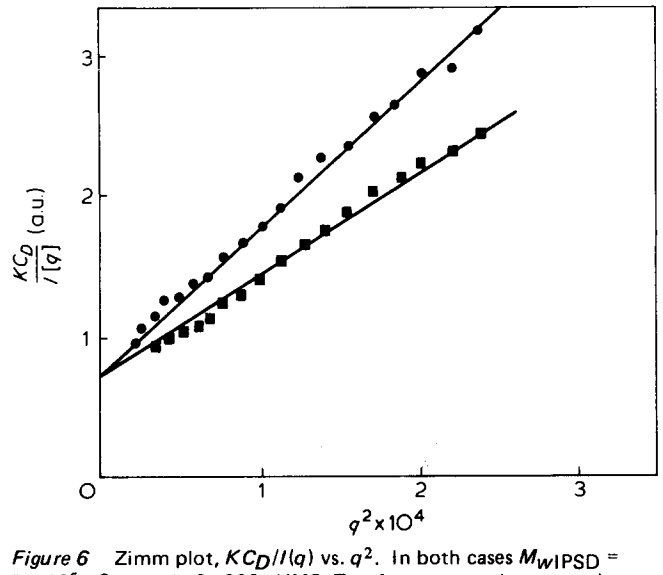

Figure 6 Zimm plot, $KC_D/I(q)$ vs. q^2. In both cases M_{wIPSD} = 5 x 10^5. ●, sample C–200–HM2; ■, reference sample prepared at 180° C, R_g = 170 Å

same for both samples. Furthermore, the accuracy of determination of the mean dimensions is quite satisfactory as shown in *Figure 7* wherein the Zimm representation is used for another tagged chain molecular weight (C-200, $M_{wIPSD} = 3 \times 10^5$).

Intermediate range. The results are detailed for each thermal treatment.

(a) Samples C-140

The neutron scattering data obtained for this range of scattering vectors are presented in a Kratky plot (*Figure 8*). The asymptotic behaviour of the form factor for labelled chains depends on the hydrogenated matrix molecular weight. In the matrix of middle molecular weight ($M_w = 4.2 \times 10^5$, HM1), q^{-2} behaviour is rapidly attained ($q^* \simeq 2.5 \times 10^{-2}$) while for the high molecular weight matrix (HM3) this behaviour is attained just beyond $q^* \simeq 7.5 \times 10^{-2}$. These results confirm those obtained in the Guinier range that show the existence of two different conformations.

(b) Samples C-140-A-180

The Kratky plots in *Figure 9* show a significant change of behaviour before (C-140) and after (C-140-A-180) annealing. These results therefore show a change of conformation as already reported in the Guinier range. For samples C-140-A-180 the q^{-2} dependence is reached for $q^* \simeq 4 \times 10^{-2}$.

(c) Samples C-200

Figure 10 shows that q^{-2} behaviour is rapidly attained for these samples ($q^* \simeq 2.5 \times 10^5$). This result is similar to that reported in a previous paper concerning samples crystallized at 185°C[4].

INTERPRETATION AND DISCUSSION

Results gathered both in the Guinier and in the intermediate ranges can now be discussed in the light of the semicrystalline models described above. For the IPS

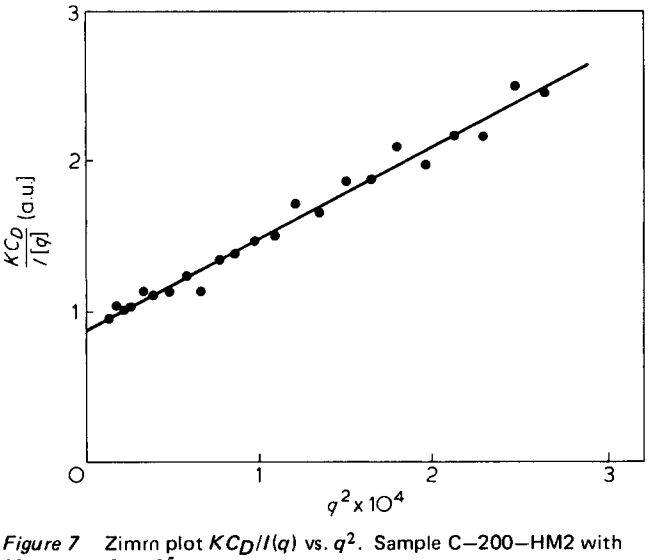

Figure 7 Zimm plot $KC_D/I(q)$ vs. q^2. Sample C–200–HM2 with M_{wIPSD} = 3 x 10^5

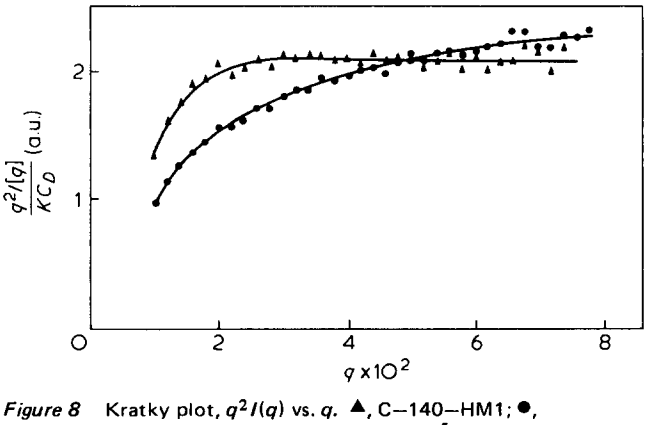

Figure 8 Kratky plot, $q^2 I(q)$ vs. q. ▲, C–140–HM1; ●, C–140–HM3. In both cases M_{wIPSD} = 5 x 10^5

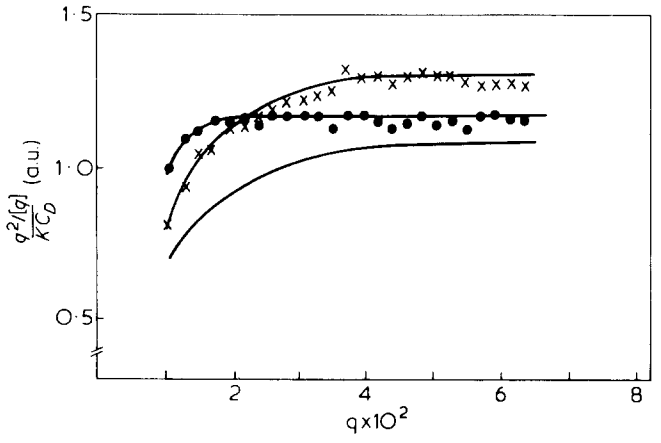

Figure 9 Kratky plot, $q^2I(q)$ vs. q. ●, Sample C–140–HM1; x, sample C–140–A–180–HM1. Full line indicates results obtained on the amorphous sample prepared in an atactic matrix at 140°C. In all cases M_wIPSD = 5 x 10^5

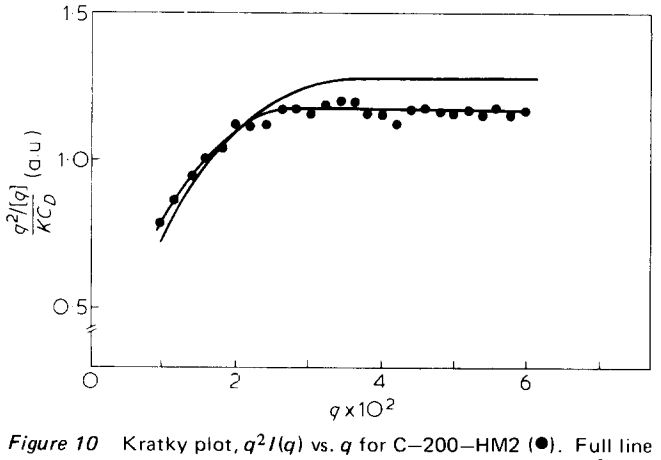

Figure 10 Kratky plot, $q^2I(q)$ vs. q for C–200–HM2 (●). Full line stands for results obtained in an atactic matrix prepared at 200°C. In both cases M_wIPSD = 5 x 10^5

samples used here, the rates of crystallization were sufficiently high that the amount of non-incorporated material is too small to have any significant influence on the scattered intensity and in particular on the mean dimensions. Thus, the calculations derived in the theoretical section are applied without correction.

Viscoelastic considerations were used in order to verify the consistency of the models. They consist[9], as mentioned in the Introduction, of comparing the long relaxation time τ_m to the time τ_p needed for the crystalline growth front to envelope the dimensions R_g of a chain ($\tau_p \simeq R_g/G$). The motion of the chains by reptation introduced for polyethylene[15,16] is negligible in the case of IPS due to bulky side groups and is ignored here.

Samples C-140

SANS results were different, depending on the molecular weight of the protonated isotactic matrix. For the intermediate molecular weight matrix (HM1) the exponent $\nu = 0.63$ suggests a conformational model possessing a central core. In *Table 2*, where the values of mean dimensions are calculated for a central core model in which the size of the central crystalline sequence depends on the labelled chain molecular weight, we note that the best fit with experimental data is for $g = 0.25$ and $f_2 = 5$ (the choice of $f_2 = 5$ will be explained below). However, as the value of g is rather small, a model in which the central core has a constant size would not lead to appreciably different results. In contrast, the ACA model would lead to much higher values of the radii of gyration.

The central core model is also supported by the asymptotic behaviour, where the value $n = 2$ has been found. This result implies that chain incorporation into the crystalline lamella occurs along the 330 plane both in the central core and in the crystalline parts located in the wings. Such a result has been already obtained under other circumstances[4,8].

For the high molecular weight matrix (HM3) the experimental exponent $\nu = 0.5$ as well as the invariance of the mean dimensions suggest a garland model. Numerical calculations performed using equation (5) by taking $\overline{R_A^2} = 4.8 \times 10^{-2}$ M [12], $l_c \simeq 70$ Å [17], $x = 0.34$, $z \simeq 0.75$[8] and $\overline{I^2}^{1/2} = 12.6$ Å [18], show that experimental results agree with $f = 3$ or $f = 5$. As the q^{-2} dependence is reached for $q^* \simeq 8 \times 10^{-2}$ in the intermediate range, we may reasonably take the value $f = 3$ according to equation (17). It must be emphasized that the use of equation (5) with $f = 1$ leads to values of mean dimensions 40% higher than those measured here. As the accuracy of determination of radii of gyration is of sufficient precision, this case must therefore be discounted.

We make use of viscoelastic properties to support the conformational models. Calculating τ_m using values given by Suzuki[19] and τ_p with $R_g \simeq 200$ Å and $G = 2.5 \times 10^{-2}$ μm min^{-1} [20], we find:

for HM1 $\tau_m \simeq 1500$ s $\tau_p \simeq 70$ s

for HM3 $\tau_m > 24$ h $\tau_p \simeq 70$ s

Comparison of these values suggests that the crystalline sequences should be very short in both cases. From neutron scattering, this is effectively the case for HM3 but not for HM1. However, we can find an explanation for this inconsistency from both d.s.c. results and the comments of Lemstra *et al.*[14]; isothermal crystallization at high supercooling gives rise to a secondary process much slower than the primary process. We may assume that the central core is located in structures arising from secondary crystallization. The exact evaluation of $\tau_{p,s}$ is not easy but its value can be close to that of τ_m. Results obtained for crystallized–annealed samples seem to confirm such an assumption.

Samples C-140-A-180

D.s.c. thermograms (*Figures 3c* and *3d*) show that the structures arising from secondary crystallization at T_c

Table 2 Values of the mean dimensions calculated from equations (7) and (8) with different values of g for the central core model with $x = 0.34$, $z \simeq 0.75$, $\overline{R_A^2} = 4.8 \times 10^{-2}$ M, $l_c \simeq 80$ Å and $\overline{I^2}^{1/2} = 12.6$ Å. Exponents ν are calculated from a mean least squares method for molecular weights ranging from $M_w = 2.5 \times 10^5$ to 7×10^5

	M_w				
g	2.5 x 10^5	3 x 10^5	5 x 10^5	7 x 10^5	ν
0.75	142	163	244	325	0.8
0.5	131	147	212	274	0.72
0.25	122	134	179	220	0.57
Exp	121	130	172	230	0.63

Table 3 Comparison of experimental values of the radius of gyration for samples crystallized at 200°C and theoretical values obtained from application of equation (2) for the ACA model with $x = 0.34$, $z \simeq 0.75$, $R_A^2 = 4 \times 10^{-2}\ M$, $l_c = 100$ Å[17] and $\overline{I^2}^{1/2} = 12.6$ Å

M_wIPSD	$R_{g,exp}$	ν_{exp}	$R_{g,th}^{ACA}$	ν_{th}
2.5×10^5	120 ± 3		115	
3×10^5	141 ± 4	0.77	134	0.85
5×10^5	206 ± 5		208	

$= 140$°C have melted after annealing at $T_{an} = 180$°C. Neutron scattering results reveal a change in conformation after this thermal treatment. The invariance of mean dimensions as well as the experimental exponent $\nu = 0.5$ also suggest a garland conformation. Using equation (5) with $R_A^2 = 4.8 \times 10^{-2}$ M, $l_c \simeq 80$ Å [17], $x = 0.38$, $z \simeq 0.75$ [8] and $\overline{I^2}^{1/2} = 12.6$ Å [4,8], the best agreement is obtained with $f = 5$. Considering the asymptotic behaviour (*Figure 9*) and in particular the value of the scattering vector at which the q^{-2} dependence is reached, we are likewise led to $f = 5$ by application of equation (17).

Since the conformation is close to the garland model we envisage (for the C-140-HM1 samples) that the central core is effectively located in the structure arising from secondary crystallization. After melting these structures at 180°C, recrystallization promotes the formation of shorter rather than longer crystalline sequences. It is difficult to crosscheck this point by dynamic viscoelastic considerations since τ_m and τ_p are not directly available in this case. Nevertheless, this assumption seems to be consistent with d.s.c. and neutron scattering results.

Finally, the interpretation of SANS data with $f = 5$ for the C-140-A-180 justifies the use of $f_2 = 5$ in the previous situation (samples C-140-HM1).

Samples C-200

D.s.c. measurements performed on these samples show that there is only one kind of crystallization process. This implies that the semicrystalline structure is homogenous in the sample. The exponent $\nu = 0.77$* as well as the increase in the radius of gyration for high molecular weight labelled chains are consistent with the predictions of the ACA model as listed in *Table 3*. The intensity scattered in the intermediate range is also in good agreement with this model. Here, dealing with the ACA conformation, we can compare the heights of the plateaux obtained in a reduced Kratky plot ($q^2 I(q)/C_D$ vs. q) of the semicrystallized sample and an amorphous sample, both containing the same deuterated chains. Experimentally we find:

$$\rho_{exp} = \frac{C_{am} I_{cry}(q)}{C_{cry} I_{am}(q)} = 0.88$$

whereas the theoretical value ρ_{th} deduced from application of equation (12) with $R_A^2 = 4 \times 10^{-2}\ M$ [12], $x = 0.34$, $z = 0.75$, $l_c \simeq 100$ Å [17] and $\overline{I^2}^{1/2} = 12.6$ Å, is:

$$\rho_{th} = 0.92$$

The SANS results are therefore consistent with the theoretical calculations derived from the ACA model both in the Guinier and the intermediate ranges.

The results and interpretations given here should be compared with previous work[4] performed on samples crystallized at 185°C for which the ACA conformation has already been proposed. This shows that such a result is quite reproducible for another crystallization temperature and another matrix molecular weight.

Looking at the relaxation time related to HM2 and the envelopment time for $R_g \simeq 200$ Å with $G = 0.14$ μm min^{-1} [20], we obtain: $\tau_m \simeq 70$ s and $\tau_p \simeq 10$ s. These time scales support the ACA model as in previous reports[4].

CONCLUSIONS

The neutron scattering results gathered in this paper on semicrystallized IPS samples do not suffer from isotopic segregation. The interpretation of the data is consequently more simple.

The study presented here completes previous work[4,8] carried out on isotactic polystyrene by extending the crystallization temperature range. Depending on the degree of supercooling, the thermal treatment and the matrix molecular weight, the SANS results are quite different both in the Guinier and in the intermediate ranges, clearly indicating the existence of different conformations. By theoretical calculation, the results may be interpreted using conformational models of semicrystallized chains. In particular, it is shown that the size of the crystalline sequences is strongly dependent on the chain mobility in the original melt. The criterion of Yoon and Flory[9] i.e. comparison of τ_m and τ_p seems to be quite satisfactory for predicting the chain conformation in the IPS bulk-crystallized state to a good approximation.

Alternatively, this paper shows that for the lowest mobility (samples C-140-HM3), the crystalline sequences involved in the garland model are made up of three rods incorporated along the 330 plane. It therefore seems impossible to have only one rod per crystalline sequence in IPS. Thus, the switchboard model may be discounted.

* We are not dealing with a straight line (see comments and explanation, ref 10). Thus, ν is a mean exponent.

REFERENCES

1 Schelten, J. *et al. Polymer* 1976, **17**, 751
2 Allen, G. and Tanaka, T. *Polymer* 1978, **19**, 271
3 Ballard, D. G. H. *et al. Macromolecules* 1980, **13**, 677
4 Guenet, J. M. and Picot, C. *Polymer* 1979, **20**, 1483
5 Yoon, D. Y. and Flory, P. J. *Polymer* 1976, **18**, 509
6 Guttman, C. M. *et al. Faraday Discuss.* No. 68, 297 (1979)
7 Guenet, J. M. *Polymer* 1980, **21**, 1385
8 Guenet, J. M. *Macromolecules* 1980, **13**, 387
9 Flory, P. J. and Yoon, D. Y. *Nature* 1978, **272**, 226
10 Guenet, J. M. and Picot, C. *Polymer* 1979, **20**, 1473
11 Guenet, J. M. *et al. J. Appl. Polym. Sci.* 1977, **21**, 2181
12 Guenet, J. M., Picot, C. and Benoit, H. *Macromolecules* 1979, **12**, 86
13 Dedeurwaerder, R. and Oth, J. M. F. *J. Chim. Phys.* 1959, **56**, 940
14 Lemstra, P. J., Schouten, A. J. and Challa, G. *J. Polym. Sci. (A-2)* 1974, **12**, 1565
15 Klein, J. *Faraday Discuss.* No. 68, 198 (1979)
16 DiMarzio, E. A. *et al. Faraday Discuss.* No. 68 210 (1979)
17 Overbergh, N., Berghmans, H. and Reynaers, H. *J. Polym. Sci. (A-2)* 1976, **14**, 1177
18 The energy required for changing a right-hand helix into a left-hand helix or *vice versa* is high in the isotactic polystyrene ($\Delta E \simeq 10$ kcal). Consequently, a chain is mainly composed of only one kind of helicity which promotes incorporation along the crystallographic plane having stems of same helicity
19 Suzuki, R. *These* University of Strasbourg (1972)
20 Keith, H. D. and Padden, F. J. *J. Appl. Phys.* 1964, **35**, 4, 1280